TISSUE ENGINEERING: Part A
Volume 15, Number 10, 2009

DOI: 10.1089/ten.tea.2008.0394

Original Article

Polyphenol-Stabilized Tubular Elastin Scaffolds for Tissue Engineered Vascular Grafts

Ting-Hsien Chuang, M.S., Christopher Stabler, B.S., Agneta Simionescu, Ph.D., and Dan T. Simionescu, Ph.D.

Tissue-engineered vascular grafts require elastic, acellular porous scaffolds with controlled biodegradability and properties matching those of natural arteries. Elastin would be a desirable component for such applications, but elastin does not easily regenerate experimentally. Our approach is to develop tubular elastin scaffolds using decellularization and removal of collagen from porcine carotid arteries (~5 mm diameter) using alkaline extraction. Because elastin is susceptible to rapid degeneration after implantation, scaffolds were further treated with penta-galloyl glucose (PGG), an established polyphenolic elastin-stabilizing agent. Scaffolds were compared *in vitro* with detergent-decellularized arteries for structure, composition, resistance to degradation, mechanical properties, and cytotoxicity and *in vivo* for cell infiltration and remodeling potential. Results showed effective decellularization and almost complete collagen removal by alkaline extraction. PGG-treated elastin scaffolds proved to be resistant to elastase digestion *in vitro*, maintained their cylindrical shapes, showed high resistance to burst pressures, and supported growth of endothelial cells and fibroblasts. *In vivo* results showed that PGG treatment reduced the rate of elastin biodegradation and controlled cell infiltration but did not hamper new collagen and proteoglycan deposition and secretion of matrix-degrading proteases. Alkali-purified, PGG-treated tubular arterial elastin scaffolds exhibit many desirable properties to be recommended for clinical applications as vascular grafts.

Introduction

Cardiovascular diseases have created a vast demand for vascular grafts to be used as by-pass shunts for myocardial and limb revascularization and as fistulae for dialysis access.[1] Artificial blood vessels made of synthetic materials have been successful in large-diameter replacements, but they fail when used in small-diameter applications (<5–6 mm) because of poor patency and early graft occlusion.[2–5] In the United States, more than 1 million vascular procedures are performed each year involving small-diameter vessels.[6]

The current criterion standard for bypass grafts is autologous veins or arteries, but healthy autograft tissue is not always available, and allografts are in high demand but short supply. Limited availability of human grafts combined with inadequate performance of small-diameter synthetic grafts make existing alternatives suboptimal.[7–9] The fabrication of tissue-engineered vascular grafts appears to hold great promise as alternative conduits.[10,11] For example, Shin'oka *et al*. reported recently on development of vascular grafts using stem cell–seeded biodegradable scaffolds and their successful implantation in pediatric patients.[12,13]

Typical tissue engineering approaches employ scaffolds and cells brought together in such a way as to restore function and facilitate regeneration of the replaced tissue. Several methods have been reported, including a completely cellular approach,[14,15] use of decellularized tissues,[16–18] and combinations of cells with natural or synthetic scaffolds,[11,19] including promising biodegradable elastomeric polymers.[10,20,21] With few exceptions, tissue engineering approaches have relied on scaffolds to provide biological and mechanical support for cells. To achieve clinical success, vascular scaffolds should exhibit adequate porosity[22] and controlled biodegradability,[23] be fully cytocompatibile[23] and capable of being repopulated and remodeled by host cells, and express lack of antigenic determinants[24] and low thrombogenicity.[25] Mechanical strength, deformability, elasticity, and compliance are essential to withstand circulatory pressures immediately after implantation to prevent early failure, as well as at later stages, during tissue remodeling.[26,27] Overall, this appears to be an "all or nothing" scenario (unless all of these requisites is fulfilled, imperfect scaffolds may be in no way suitable for clinical use).

Scaffolds composed of purified or reconstituted extracellular matrix proteins and decellularized arteries have been widely used in tissue engineering. Natural arteries are made of concentric layers of elastin sheets interspersed with a collagen fiber network and populated by smooth muscle cells.[28] Although pure elastin has found limited applications,[29,30] the vast majority of studies have focused on the

Department of Bioengineering, Clemson University, Clemson, South Carolina.

fabrication of collagen scaffolds combined with various procedures for the formation of pores followed by seeding with cells.[31–33] However, collagen scaffolds display poor mechanical properties, including lack of elasticity.[26,34] Processed vascular tissues have been employed for tissue engineering, mostly by removal of cells (decellularization), which is necessary to remove potential antigenic determinants. Studies show poor cell infiltration in decellularized aorta upon implantation, possibly because of insufficient porosity and the dense structure of the arteries.[35] Overall, thrombosis, poor remodeling, and inadequate mechanical properties have hampered most approaches described.[11]

In view of these results, our novel approach was to selectively remove cells and collagen from decellularized porcine arteries with the purpose of creating a high density of adequately sized pores within elastin-rich scaffolds. Elastin fibers are extracellular matrix proteins that endow vascular tissues with resilience, permitting long-range deformability without energy input.[36] These properties are critical to the function of arteries, which undergo cyclical extension and recoil and would hypothetically be beneficial for tissue-engineered vascular grafts. Elastin is a naturally cross-linked, highly hydrophobic protein that rarely undergoes remodeling.[37] A contributing factor to longevity of elastin is its relative resistance to proteolysis by all but a limited number of proteases such as elastase and matrix metalloproteinases (MMPs) that are capable of degrading the mature protein. Because of its stability and low natural turnover, once elastin is degraded, *de novo* elastin formation is difficult to achieve. Unless elastin is stabilized, degeneration and calcification may occur upon implantation.[38] It is our hypothesis that stabilization of elastin scaffolds against the action of elastase would significantly improve their performance as vascular grafts. For this purpose, we are proposing to employ the unique properties of phenolic tannins as elastin-stabilizing agents.

Penta-galloyl glucose (PGG) is a derivative of tannic acid, a naturally derived polyphenol present in a wide variety of plants. Polyphenols have a hydrophobic internal core and numerous external hydroxyl groups. By virtue of this structure, they react with proteins, specifically binding to hydrophobic regions but also establishing numerous hydrogen bonds, showing particularly high affinity for proline-rich proteins such as collagen and elastin.[39,40] In addition, they are efficient antibacterial agents and reduce inflammation and antigenicity.[41] We have shown that phenolic tannins bind strongly and specifically to aortic elastin and, in doing so, render elastin highly resistant to degeneration by elastases.[42] Treatment of aortic tissue with phenolic tannins reduced elastin-associated calcification when tested in a subdermal implantation animal model.[38] Local delivery of PGG to rat abdominal aorta prevented aneurysm formation in the absence of changes in serum liver enzyme activities or liver histology, clearly showing that PGG was not toxic at local or systemic levels.[43] Moreover, extractables obtained from PGG-fixed tissues exhibited low *in vitro* cytotoxicity toward fibroblasts and smooth muscle cells[44] and thus can possibly be used safely in tissue engineering applications.

Here, we describe development of a tissue-engineered construct that benefits from the natural architecture of the artery and is composed of a PGG-stabilized network of porous vascular elastin. We show that these scaffolds exhibit excellent biological and mechanical properties and are clearly superior to decellularized arteries in terms of cell infiltration and remodeling potential.

Materials and Methods

Materials

High-purity 1,2,3,4,6-penta-O-galloyl-beta-D-glucose (PGG) was a generous gift from N.V. Ajinomoto OmniChem S.A. (Wetteren, Belgium; www.omnichem.be). Pure DNA, ribonuclease, glutaraldehyde (50% stock), and collagenase type VII from *Clostridium histolyticum* were all purchased from Sigma-Aldrich Corporation (St. Louis, MO). Deoxyribonuclease I was from Worthington Biochemical Corporation (Lakewood, NJ), and bicinchoninic acid (BCA) protein kits from Pierce Biotech (Rockford, IL). Electrophoresis apparatus, chemicals, and molecular weight standards were from Bio-Rad (Hercules, CA), and elastase was from Elastin Products Company (Owensville, MO). All other chemicals were of highest purity available and typically obtained from Sigma Aldrich.

Scaffold preparation. Fresh porcine carotid arteries (60–80 mm long, 5–6 mm in diameter) obtained from Animal Technologies, Inc. (Tyler, TX) were processed for elastin scaffold preparation using two methods. The first involved incubation of arteries in 0.1 M of sodium hydroxide (NaOH) solution at 37°C for 24 h and then extensive rinsing with deionized water until pH dropped to neutral. This treatment removes all cells and most of the collagen, leaving vascular elastin intact (referred to as "elastin scaffolds"). The second method employed 24 h of hypotonic shock; extraction with 0.25% sodium-deoxycholate, 0.15% Triton X-100, 0.1% ethylenediaminetetraacetic acid, and 0.02% sodium azide in 50 mM Tris–hydrochloric acid (HCl) buffer (pH 7.8) with mild agitation for 6 days at 22°C; and changes of the solution after 3 days. After rinsing with double-distilled water and 70% ethanol to remove detergents, tissues were treated with a deoxyribonuclease/ribonuclease mixture (360 mU/mL for each enzyme) at 37°C. This treatment removes all cells but leaves vascular collagen and elastin fibers intact (referred to as "detergent-decellularized artery").

Scaffold characterization. For histological evaluation, paraffin-embedded samples were stained with hematoxylin and eosin (H&E), Gomori's one-step trichrome, and Verhoeff van Gieson (VVG) stain ($n = 4$ slides per group per stain). Digital pictures were taken of H&E-stained samples ($n = 2$ slides per group) at 400× magnification, and pore sizes between intact elastin fibers were measured using AxioVision Release 4.6.3 digital imaging software (Carl Zeiss Micro Imaging, Inc., Thornwood, NY).

To validate decellularization, total genomic DNA was extracted and purified ($n = 3$ per group) using a Fibrous Tissue DNeasy Kit (Qiagen, Valencia, CA) following the manufacturers' instructions. DNA samples were subjected to agarose and ethidium bromide gel electrophoresis alongside pure DNA standards (10 – 100 ug/mL) followed by densitometry using Gel-Pro Analysis Software (MediaCybernetics, Silver Spring, MD). DNA levels were calculated from the standard curve and normalized to initial tissue wet weight.

Chemotaxis assays were conducted using a Boyden chamber (NeuroProbe, Gaithersburg, MD) and a polycarbonate filter with 8-μm diameter pores, as per the manufacturer's

instructions. Soluble elastin peptides were prepared by treatment of elastin scaffolds with ultrapure elastase (10 U/mL in 50 mM Tris buffer, 1 mM calcium chloride, 0.02% sodium azide) for 24 h. The supernatant was filtered through (Microcon YM-3 centrifugal devices, Millipore, Billerica, MA) and peptides smaller than 3 kDa were collected in the flow-through for chemotaxis assays. Rat aortic fibroblasts and, separately, rat aortic smooth muscle cells (1×10^6/well, prepared in house using collagenase/explant techniques) suspended in Dulbecco's modified Eagle medium (DMEM) and 0.1% bovine serum albumin were used in these tests; undiluted fetal bovine serum (FBS; 100%) was used as a positive control, and DMEM and 0.1% bovine serum albumin as the negative control. Cells migrated for 4 h at 37°C and 5% carbon dioxide (CO_2). After incubation, the nonmigrated cells were removed using a wiper blade (NeuroProbe, Gaithersburg, MD) and the filter fixed and stained using a DiffQuick kit (Dade Behring Inc, Newark, DE), dried, and screened for migrated cells using an inverted microscope. Results were reported as negative (0–2 cells per 10× field), slightly positive (2–10 cells per 10× field), or positive (>10 cells per 10× field).

Scaffold stabilization and *in vitro* testing. Elastin scaffolds were treated for 24 h at room temperature with 0%, 0.075%, 0.15%, 0.3%, and 0.6% PGG in 50 mM dibasic sodium phosphate buffer in saline with 20% isopropanol, pH 5.5. Samples ($n=6$ per group) were lyophilized; weighed; treated with 10 U/mL of elastase in 50 mM Tris buffer, 1 mM of calcium chloride, and 0.02% sodium azide at 37°C for 48 h; and then rinsed exhaustively and lyophilized to record dry weight after elastase. The difference in dry weight was used to calculate percentage mass loss. Resistance to elastase was also compared with that of detergent-decellularized arteries.

To test for cytotoxicity, 1-cm^2 samples cut from 0.3% PGG-treated scaffolds ($n=3$ per stain) were rinsed in phosphate buffered saline for 72 h, incubated overnight in 50% FBS in culture medium, and seeded with $30\times10^3/cm^2$ porcine endothelial cells and separately with fibroblasts. After 7 days of cell culture and one medium change, cell-seeded scaffolds were stained with DiffQuick kit (Dade Behring Inc., Newark, DE), 4′,6-diamidino-2-phenylindole, and Live/Dead (Promega, Inc.) stains.

Burst pressures were determined using a peristaltic pump and a piezoelectric pressure transducer (Endevco, San Juan, CA) connected to a personal computer through a universal serial bus–interfaced data-acquisition module (Omega Engineering Inc., Bridgeport, NJ). Tubular scaffolds ($n=6$ per group) were measured using digital calipers and mounted using plastic ties onto polyethylene connectors, and physiologic saline pressure build-up was created by gradually increasing the speed of the peristaltic pump. Voltage signal outputs were recorded using LabView (National Instruments Corporation, Austin, TX) and transformed into mmHg. Burst pressures were recorded for elastin scaffolds and compared with those of fresh carotid arteries and detergent-decellularized arteries.

For compliance testing, a similar setup was used as for burst pressure in which tubular scaffolds were subjected to 80 and 120 mmHg using a column of hydrostatic pressure, with pressures measured using the transducer and external diameters measured using digital photography in six places along the mid-portion of the graft ($n=6$ samples per group). Compliance was calculated as the difference in diameter increase at the two pressures and expressed as a percentage.

For tensile testing, samples were cut into 5-×50-mm dumbbell shapes in the longitudinal direction of the blood vessel, and thickness was measured using digital calipers and analyzed at a constant uniaxial velocity of 0.1 mm/s until failure using a 10-Newton load cell on a Synergie 100 testing apparatus (MTS Systems Corporation, Eden Prairie, MN). Stress was calculated by dividing the load by tissue cross-sectional area and results expressed as stress–strain curves. Elastic modulus (slope at specific strain ±4 data points) was calculated at 20%, 40%, and 60% and at rupture for all samples and results compared using analysis of variance (ANOVA) statistical analyses.

In vivo *evaluation*

Three sample groups were prepared as follows: control untreated elastin scaffold, PGG-treated elastin scaffold (0.3% PGG), and detergent-decellularized arteries. Samples were cut into 5-×20-mm shapes and rinsed in sterile saline before implantation. Male adult Sprague-Dawley rats (weighing ~250 g, Harlan Laboratories, Indianapolis, IN) were sedated with acepromazine (0.5 mg/kg, Ayerst Laboratories, Rouse Point, NJ) and maintained on 2% isoflurane during surgery. A small transverse incision was made on the backs of the rats, and two subdermal pouches (one superior and one inferior to the incision) were created. Samples were implanted into the subdermal pouches ($n=6$ implants per group per time point) and incisions closed with surgical staples. After surgery, the rats were allowed to recover and permitted free access to water and food. The Animal Research Committee at Clemson University approved the animal protocol, and National Institutes of Health guidelines for the care and use of laboratory animals (publication #86-23 Rev. 1996) were observed throughout the experiment.

Rats were humanely euthanized using CO_2 asphyxiation at 4 and 8 weeks after surgery and samples retrieved for analysis. A small section of each explant with its associated capsule was fixed for histological evaluation. The remainder of the explants were cleaned free of capsule using microdissection, rinsed in saline, and then divided for analysis.

For DNA analysis, explants ($n=3$ per group) were weighed, and total genomic DNA was extracted and purified using the Qiagen kit described above. Content of pure DNA was measured using ultraviole spectrophotometry at 260 nm with background correction at 320 nm. DNA levels were calculated from a standard curve and expressed as ng/mg wet weight.

For histology, samples were placed in formalin and paraffin sections (5 μm) were stained with H&E, Gomori's one-step trichrome, and VVG ($n=6$ slides per group per stain). Two independent investigators measured cell infiltration depth on H&E- and trichrome-stained slides ($n=3$ slides per group per time point) using AxioVision Release 4.6.3 digital imaging software (Carl Zeiss MicroImaging, Inc.). Results were expressed as % ± standard error of the mean (SEM) of total scaffold thickness. Cell density in areas infiltrated by cells (outside one-third of each section) was measured on H&E-stained sections by digitally overlaying a 50-×50-um grid and counting cell nuclei within the grid ($n=10$ measurements per group). Results were expressed as cell density (mean number of cells/250 um^2 area ± SEM).

For immunohistochemical identification of infiltrating cell types, sections were exposed to 0.1% proteinase K solution

(25 U/500 mL, Qiagen DNeasy Tissue Kit) in Tris buffered saline (TBS), pH 7.5 at 22°C for 30 s. Endogenous peroxidases were blocked with 0.3% hydrogen peroxide in 0.3% normal sera (Vectastain Elite ABC kit for rabbit immunoglobulin (Ig)G, Vector Laboratories, Burlingame, CA). Sections were immunostained using mouse anti-rat monoclonal antibodies to alpha-smooth muscle cell actin (1:200, Sigma), macrophages (1:200, Chemicon, Temecula, CA), vimentin (1:200 dilution, Sigma), CD8 (1:200, Sigma), and active prolyl-4-hydroxylase (1:200 dilution, Chemicon) at 22°C for 1 h. To minimize cross-reactivity, rat-absorbed biotinylated anti-mouse IgG was used in place of the biotinylated secondary antibody provided with the staining kit. Negative staining controls were performed with the omission of the primary antibody. A diaminobenzidine tetrahydrochloride peroxidase substrate kit was used to visualize the specific staining (Vector Laboratories), and sections were lightly counter-stained with hematoxylin. Positively stained cells (dark brown) were counted on each section and expressed as percentage of total reactive cells. As positive immunohistochemistry controls, we also stained paraffin sections from rat spleen (macrophage and lymphocyte control) and rat skin (alpha-smooth muscle cell actin, fibroblast and prolyl-4-hydroxylase controls) in parallel with the explant sections.

To visualize phenolic groups, PGG-fixed scaffolds were stained *en bloc* with ferric chloride, embedded in Tissue Tek OCT compound (Sakura Finetek, USA Inc., Torrance, CA) and 6-μm-thick sections counterstained with light green. PGG appears brown with this staining.[43] Non-implanted PGG-treated scaffolds were also stained for comparison.

For detection of MMPs in explanted scaffolds, proteins were extracted in 50 mM Tris, 1% Triton X-100, 0.1% sodium dodecyl sulfate, 1% sodium deoxycholate, and 150 mM sodium chloride with protease inhibitor mixture, pH 7.4 buffer, and protein content was determined using BCA assay as described before[43] and subjected to gelatin zymography using 4 μg of protein per lane alongside molecular weight standards. For comparison, extracts prepared from fresh carotid artery, unimplanted elastin scaffolds and PGG-treated un-implanted elastin scaffolds were analyzed in parallel with explanted samples. MMP-2 and MMP-9 were identified according to their relative molecular weights (68–72 kDa and 90–92 kDa, respectively). Intensity of MMP bands (white bands on dark background) was evaluated according to densitometry using Gel-Pro Analysis Software (Media Cybernetics, Silver Spring, MD) and expressed as relative density units normalized to protein content.

For calcification analysis, explanted samples ($n = 4$ per group per time point) were rinsed in saline, lyophilized to obtain dry weight, and individually hydrolyzed in 6 N HCl, dried under nitrogen, and reconstituted in 1.0 mL of 0.01 N HCl. Calcium content was then measured using atomic absorption spectrophotometry as described before.[45–47]

For quantification of proteoglycans, samples were treated with papain overnight, and glycosaminoglycans (GAGs) released into solution were assayed with 1,9-dimethylmethylene blue reagent using a 0- to 1.25-ug chondroitin sulfate standard curve, as described by Hoemann *et al.*[48]

Statistics

Results are represented as means ± SEMs. Statistical analysis was performed using one way Analysis of Variances (ANOVA), and results were considered significantly different at $p < 0.05$.

Results

Characterization of elastin scaffolds

We used a novel alkali extraction method for preparing elastin scaffolds from porcine carotid arteries. Histological analysis confirmed complete decellularization, almost complete collagen removal, and presence of spindle-shaped pores averaging 15 to 30 μm wide and 20 to 70 μm long interspaced between intact elastin fibers (Fig. 1). Decellularization was also confirmed according to DNA extraction and agarose gel electrophoresis (Fig. 2A), which showed a more than 96% reduction in DNA content. Decellularization was not complete with the detergent extraction method, which required extensive and repetitive exposure to nucleases for effective cell removal (Fig. 2). The alkali extraction method was also shown to result in tubular elastin scaffolds that maintained the three-dimensional cylindrical architecture of the artery, easily supporting its own weight (Fig. 2B). Furthermore, tubular scaffolds were easy to handle and suture to native arteries (ongoing animal implants, data not shown). Smooth muscle cells and fibroblasts exhibited strong positive chemotaxis toward peptides obtained from elastase-treated scaffolds (Fig. 2C–F), suggesting that scaffold degradation would encourage cell migration and repopulation of implanted scaffolds.

Scaffold stabilization

To optimize elastin stabilization, tubular vascular elastin scaffolds were treated with different PGG concentrations and subjected to elastase digestion (Fig. 3A). Untreated elastin scaffolds degraded almost completely in elastase, indicating that the scaffold was inherently biodegradable. As PGG concentration increased, there was a significant decrease in mass loss, reaching a plateau at approximately 0.3% PGG. Thus, we chose treatment of elastin scaffolds with 0.3% PGG. In a second experiment, resistance to elastase of the PGG-treated scaffolds was compared with those of detergent-extracted arteries (Fig. 3B, C). Results showed that detergent-decellularized arteries were as degradable as alkali-extracted arteries and that PGG interacts with elastin fibers within the scaffold and renders them resistant to enzymatic degradation.

Direct-contact cytotoxicity tests showed that alkali-purified elastin scaffolds were cell friendly and that PGG treatment did not render the scaffold cytotoxic (Fig. 3D). Endothelial cells and fibroblasts attached and spread onto the surface of scaffolds without visible signs of cell death.

In vitro analysis (Fig. 4A) showed burst pressures of fresh carotid arteries at approximately 2000 mmHg, values that were not significantly different from those of detergent-decellularized arteries ($p > 0.05$). Vascular elastin scaffolds obtained using alkaline extraction exhibited mean burst pressures values of 630 mmHg ($p < 0.05$ compared with fresh artery). After PGG treatment, burst pressure values increased to more than 800 mmHg, but these values were not statistically different from those for untreated elastin scaffolds ($p > 0.05$). Most elastin scaffolds exhibited similar burst patterns, with circumferential ruptures predominating over longitudinal tears (Fig. 4B).

Vascular elastin scaffolds showed distensibility similar to that of fresh arteries at low strains and lower ultimate stress at

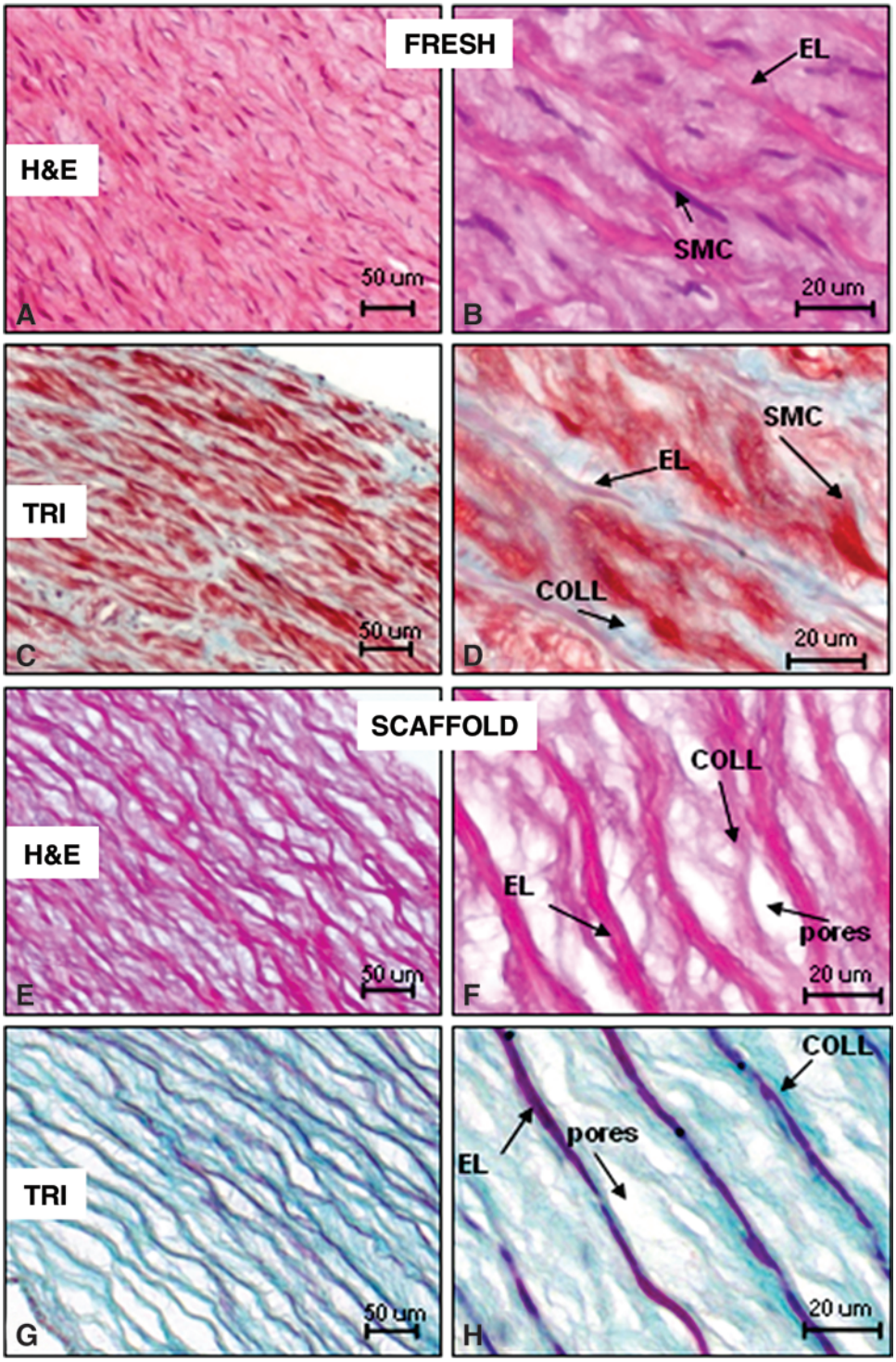

FIG. 1. Characteristics of acellular porcine elastin scaffolds derived from carotid arteries. (**A**) H&E staining of native arteries showing overall histology. (**B**) Higher magnification showing smooth muscle cells (SMCs) and elastin fibers (ELs). (**C**) Trichrome stain of native arteries showing overall aspect and (**D**) at higher magnification showing SMCs, Els, and collagen fibers (COLL, blue). (**E**) Elastin scaffolds showing porous structure by H&E stain, which at higher magnification, (**F**) reveals complete absence of cells and some collagen remnants within the inter-fibrillar pores. (**G–H**) Trichrome staining of the elastin scaffolds shows typical elastin fibers (dark red) with some weak collagen staining (blue), and absence of cells. Color images available online at www.liebertonline.com/ten.

higher strains (Fig. 4C). PGG fixation changed the shape of the curve and showed stiffening of the scaffolds at low strains while maintaining similar slopes at higher strain levels. For example, at 20% strain, the elastic moduli were 0.11 ± 0.01 MPa for control, 0.20 ± 0.02 MPa for 0.15% PGG, and 0.49 ± 0.03 MPa for 0.3% PGG (all values statistically different, $p < 0.05$). All samples failed by rupture at approximately 1.5 ± 0.7 MPa ($p > 0.05$), indicating that neither decellularization nor PGG fixation influenced overall tissue tensile strength.

Extensibility testing at 80 and 120 mmHg showed $7.5 \pm 2\%$ compliance for fresh arteries and $20 \pm 4\%$ for elastin scaffolds. However, after PGG treatment, the compliance decreased to almost physiologic levels of $9.5 \pm 1\%$ (not statistically different from fresh arteries, $p > 0.05$).

Taken together, the data show that PGG reduced distensibility and stiffened vascular elastin scaffolds, indicating that PGG interacts with elastin fibers within the aortic tissue without affecting cytotoxicity.

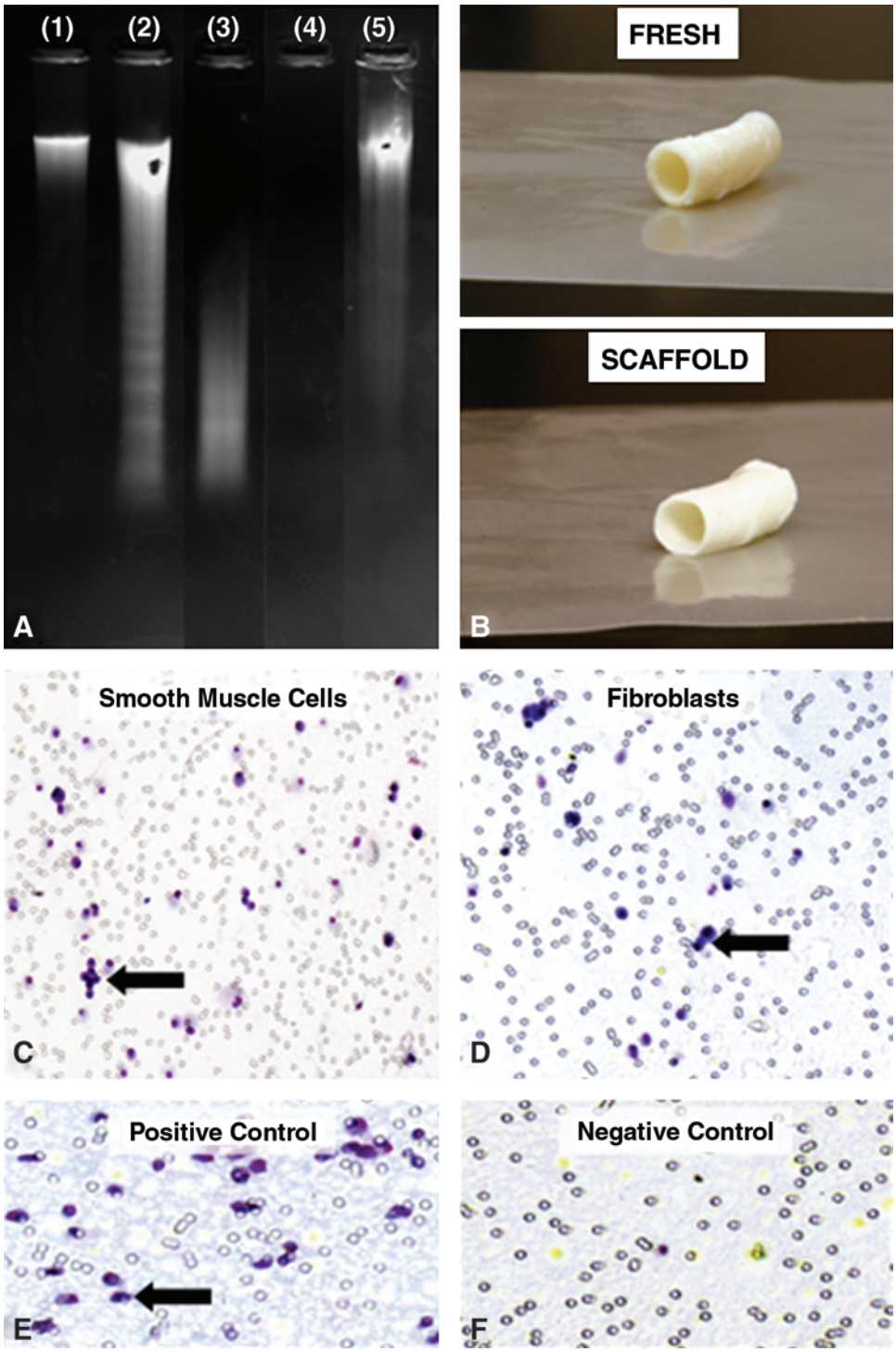

FIG. 2. Properties of elastin scaffolds: (**A**) Agarose/ethidium bromide gel electrophoresis of whole genomic DNA extracted from fresh carotid arteries (lane 1), detergent-extracted arteries after first (2) and second extraction (3), alkali-extracted carotid arteries (4) showing complete lack of DNA and a genomic DNA standard (5). (**B**) Macroscopic aspects of fresh arteries and alkali-extracted arteries. (**C**) Chemotaxis of smooth muscle cells and (**D**) fibroblasts for peptides obtained by elastase digestion of alkali-extracted elastin. Black arrows are pointing at one of many migrated cells. (**E**) Positive chemotaxis control, (**F**) Negative chemotaxis control. Color images available online at www.liebertonline.com/ten.

Biocompatibility testing

Control untreated elastin scaffolds, PGG-treated elastin scaffolds, and detergent-decellularized arteries were analyzed at 4 and 8 weeks post-implantation. Histological analysis of 4-week explants showed that all scaffolds were generally cell friendly, with host cells migrating inward from both sides (adventitia and intima) and repopulating the scaffolds gradually (Fig. 5A). An exception was the detergent-decellularized arteries group, which showed limited cell infiltration at both time points. Areas of cell infiltration coincided with significant degeneration of the elastic fibers (VVG stain, Fig. 5B), which were apparently replaced by new collagenous fibers, as evidenced by trichrome stain (Fig. 5A). By 8 weeks, extensive inward cell repopulation and remodeling had taken place in control untreated elastin scaffolds, as seen by almost complete cell infiltration and complete disappearance of the elastin fibers, suggesting that elastin is indeed a biodegradable scaffold (Fig. 5C, D). In PGG-treated elastin scaffolds, repopulation and elastin degradation had advanced inwards by approximately

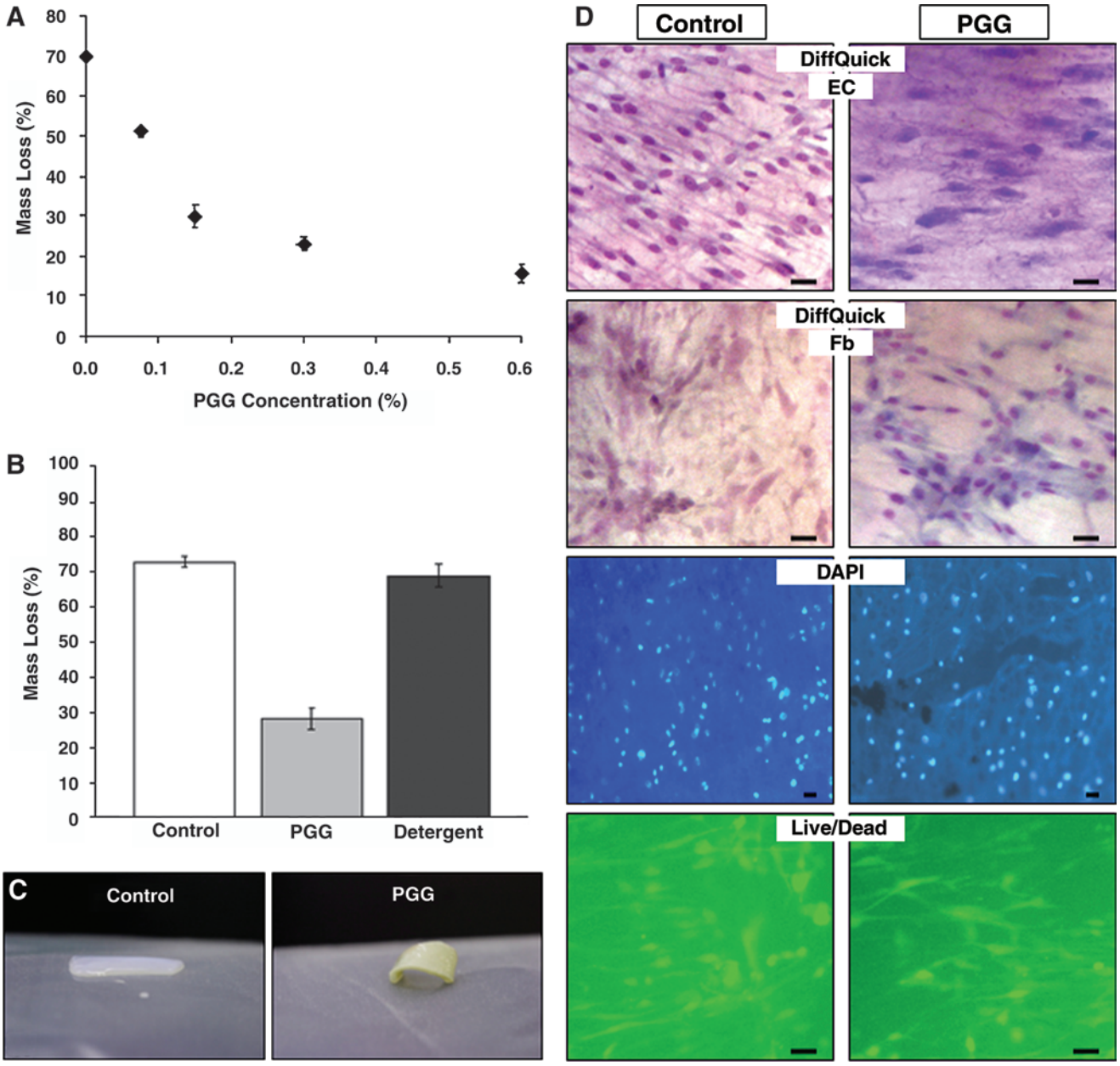

FIG. 3. Stabilization of elastin scaffolds. (**A**) Resistance to elastase of penta-galloyl glucose (PGG)-treated elastin scaffolds; a concentration study. Percentage mass loss after elastase treatment is shown for untreated scaffolds and those treated with increasing PGG concentrations. All values were statistically different (analysis of variance, $p < 0.05$). (**B**) Comparison of resistance to elastase for the three main scaffold groups before implantation, untreated elastin scaffolds (control), 0.3% PGG-stabilized scaffolds (PGG), and detergent-decellularized arteries (detergent). (**C**) Macroscopic aspect of elastase-treated samples of control untreated elastin scaffolds (left) and PGG-treated elastin scaffolds (right). (**D**) Cytotoxicity of scaffolds was tested by seeding endothelial cells (ECs) and fibroblasts (Fbs) separately on 0.3% PGG-treated scaffolds (PGG) and untreated scaffolds (control). Cells growing on the surfaces were stained with DiffQuick to show nuclei and cytoplasm, with 4′,6-diamidino-2-phenylindole for nuclear DNA stain (blue fluorescence) and with live/dead stain (live cells stain green and dead cells red). All bars are 20 um. Color images available online at www.liebertonline.com/ten.

one-third from each side at 8 weeks, leaving an intact inner "core" of elastin fibers that was not repopulated or remodeled by host cells. The outer areas exhibited well-organized, newly laid down collagen fibers, as shown by trichrome stain. VVG stain confirmed these observations, showing less *in vivo* degeneration of elastin fibers in the PGG-treated samples (Fig. 5D). These data indicate that alkali-mediated decellularization of arteries is more conducive to cell repopulation than detergent-based methods and that PGG treatment of vascular elastin has the potential to limit or control scaffold degradation, repopulation, and remodeling.

These results were confirmed by measurements of DNA content (Fig. 6A), which correlated with progressively more cell numbers in all groups, fewer cells in detergent-decellularized tissues, and intermediate cell numbers in PGG-treated elastin scaffolds (all values were different at 8 weeks, $p < 0.05$). Cell

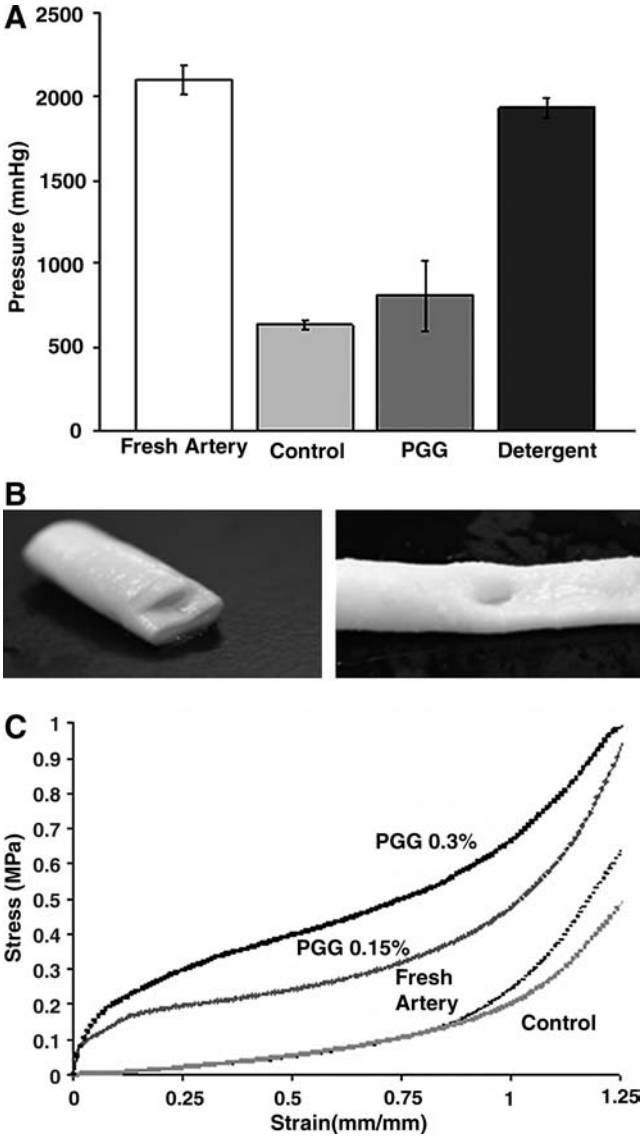

FIG. 4. Mechanical properties of elastin scaffolds. (**A**) Burst pressures for fresh carotid arteries, untreated elastin scaffolds (control), 0.3% PGG-stabilized scaffolds (PGG) and detergent-decellularized arteries (detergent). (**B**) Representative macroscopic pictures showing two patterns observed during burst pressure analysis, radial tears (left) and longitudinal tears (right) of elastin scaffolds. (**C**) Representative stress–strain curves for fresh carotid arteries, untreated elastin scaffolds (control), and 0.15% and 0.3% PGG-stabilized elastin scaffolds.

infiltration depth, calculated as the sum of adventitial and intimal depths and expressed as percentage of cell-infiltrated distance of total thickness, is shown in Figure 6B. In all samples, infiltration through the adventitia was almost twice as extensive as through the intima (data not shown). Data obtained at 4 weeks of implantation showed similar levels in all implant groups (>30% infiltration depth), except in the detergent-decellularized arteries, which was significantly lower ($21 \pm 2\%$, $p < 0.05$). After 8 weeks of implantation, the control untreated elastin scaffold was almost fully infiltrated with cells ($93 \pm 2\%$), whereas PGG-treated elastin showed significantly less infiltration ($72 \pm 2\%$, $p < 0.05$). After 8 weeks, the detergent-decellularized arteries showed infiltration values similar to those of the 4-week implants ($21 \pm 2\%$), indicative of limited potential for cell infiltration in these samples. Cell density measured in the infiltrated areas showed a similar trend as infiltration depth, namely high density in control untreated elastin scaffolds and intermediate cell density in PGG-treated elastin scaffolds (Fig. 6C).

To evaluate potential for remodeling, we analyzed MMP activities in explants and compared them with activities in fresh carotid aorta and unimplanted control elastin scaffolds (Fig. 6D). Elastin scaffolds exhibited lower MMP levels than fresh tissue, indicating that decellularization may remove most protease activities. Practically no MMP activity could be detected in PGG-treated scaffolds, indicating that PGG has the potential to inhibit MMPs. After 4 weeks of implantation, MMP levels were more than 10 times greater than unimplanted scaffold levels (Fig. 6D). Conversely, MMP levels were approximately 50% lower in PGG-treated scaffolds at 4 weeks. Similar MMP levels were obtained after 8 weeks of implantation, indicating that PGG treatment has the potential to control MMP activity after scaffold implantation. GAG content analysis showed that neither NaOH nor detergent-decellularized arteries had lost any detectable GAGs after cell-removal treatments (Fig. 6E, $p > 0.2$). After 4 and 8 week of implantation, GAG levels had increased significantly in treated and untreated elastin scaffolds, suggesting that infiltrating cells had deposited newly synthesized proteoglycans.

Immunohistochemical studies showed that infiltrating cells were positive for vimentin, alpha-smooth muscle cell actin, and macrophage antibodies and negative for cytotoxic lymphocyte antibodies (Fig. 7A). A similar pattern was seen at 8 weeks, suggesting that activated fibroblast infiltration could be chronic in these implants and could lead to remodeling and regeneration in vascular tissues. As further proof of remodeling, a large number of infiltrating cells were also positive for prolyl-4-hydroxylase, an enzyme actively involved in synthesis of new collagen fibers (Fig. 7B). Semi-quantitative analysis of explants obtained at 4 weeks revealed larger numbers of macrophages in untreated scaffolds than in PGG-treated scaffolds, whereas at 8 weeks, both scaffolds showed similar cell-type distribution (Fig. 7C).

Phenol staining of PGG-treated elastin scaffolds showed discrete binding of PGG to every elastic fiber, mainly decorating the surface of the fibers (Fig. 7C). This binding pattern was well preserved after 4 and 8 weeks of implantation, suggesting that PGG–elastin bonds are stable for at least 8 weeks *in vivo*.

Quantification of calcium in explants (Table 1) revealed that untreated elastin scaffolds accumulated significant amounts of calcium (>100 ug/mg dry), whereas PGG-treated elastin did not deposit any detectable calcium salts at 4 weeks (1.4 ug/mg dry) and little at 8 weeks (4.4 ug/mg dry), suggesting that calcification may not be a major concern in PGG-stabilized elastin scaffolds implanted as vascular grafts. Finally, detergent-decellularized arteries did not accumulate any significant calcium in our system.

Discussion

Decellularization is an essential step in scaffold preparation for tissue engineering because it serves to remove antigenic

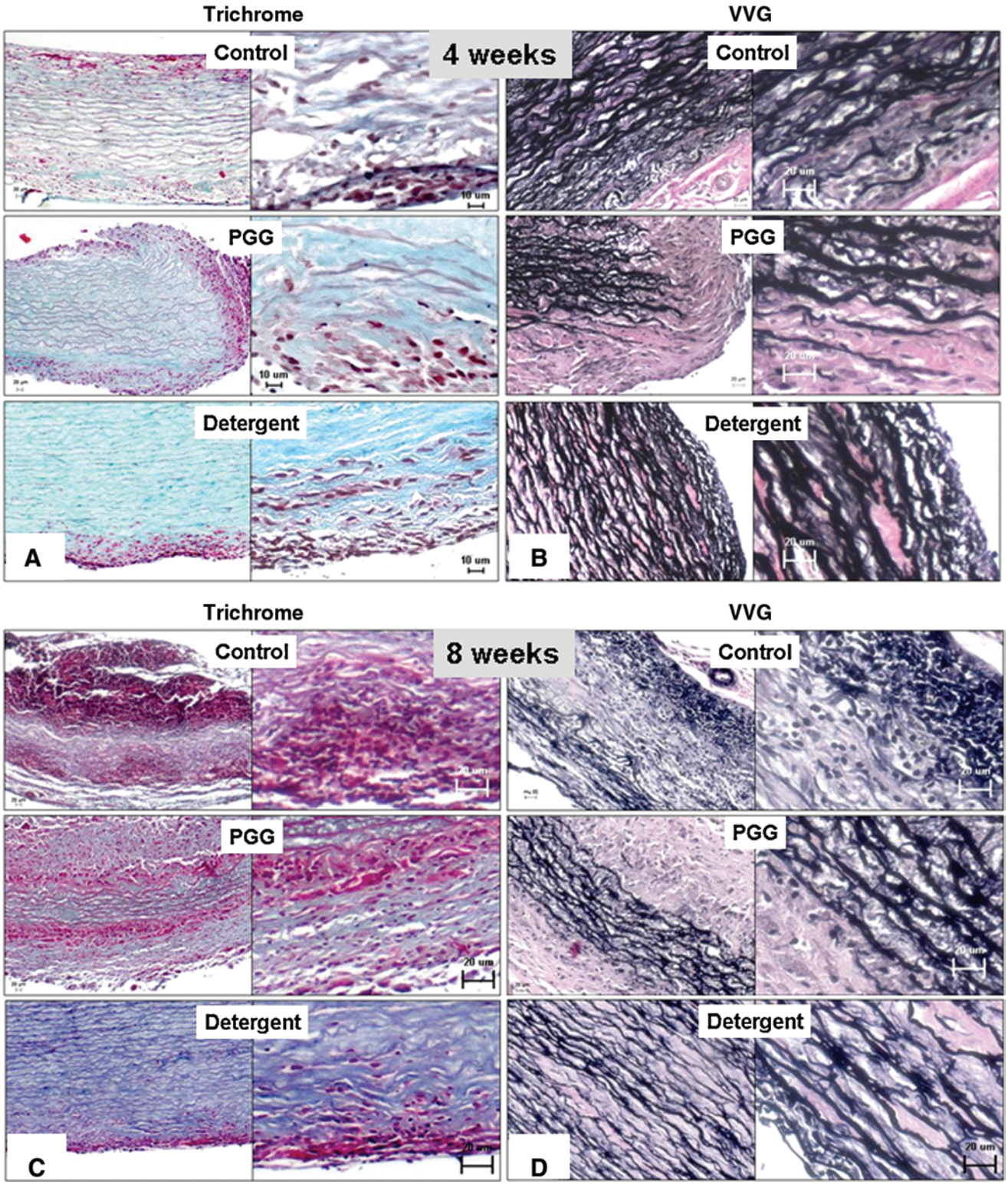

FIG. 5. Histological analysis of subdermally implanted scaffolds. Representative micrographs showing 4-week explants (**A** and **B**) and 8 week explants (**C** and **D**) stained with trichrome stain (**A** and **C**) where elastin stains dark red, collagen blue and cells pink, and Verhoeff van Gieson stain (**B** and **D**), where elastin stains black and non-elastin components pink. Samples are shown at lower magnification (micrographs on left of each panel) and higher magnification (on right). Color images available online at www.liebertonline.com/ten.

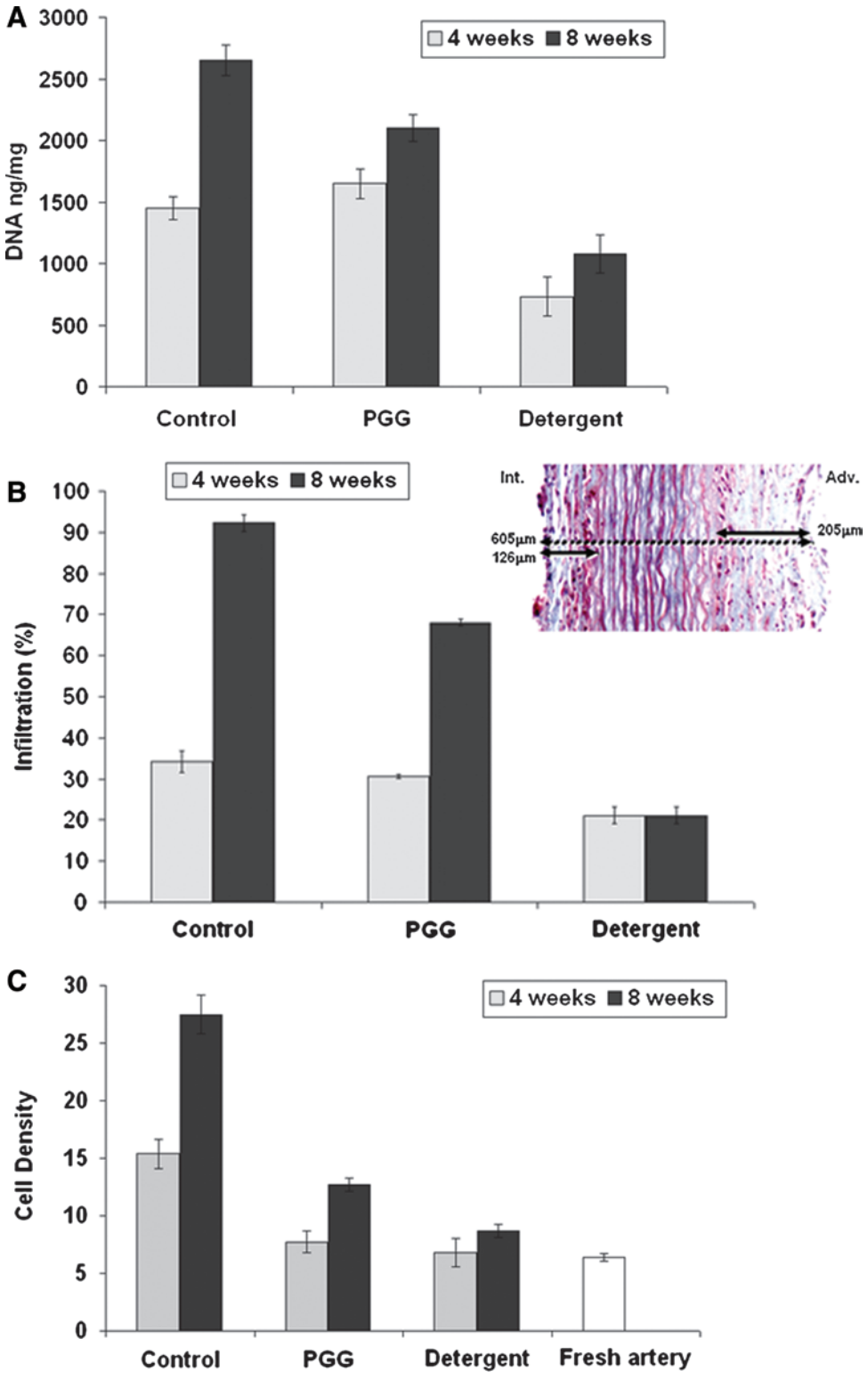

FIG. 6. Cell infiltration and remodeling activities in implanted scaffolds. Groups analyzed were alkali-purified elastin scaffolds (control), 0.3% PGG-stabilized elastin scaffolds (PGG), and detergent decellularized scaffolds (detergent) before and after 4 weeks (4w) and 8 weeks (8w) of implantation. (**A**) DNA content in explants. Whole genomic DNA was purified from explants and quantities expressed as ng/mg wet tissue. (**B**) Infiltration depth expressed as percentage of total scaffold thickness. Insert shows a representative trichrome-stained section labeled with actual measurements of cell infiltration (full double arrows) through the intima (Int.), adventitia (Adv.), and scaffold thickness (dashed double arrow). (**C**) Cell density measured in infiltrated areas expressed as cell numbers/area of 250 um^2. Cell density in fresh carotid artery is also shown for comparison. (**D**) Matrix metalloproteinase (MMP) activities measured by gelatin zymography and reported as relative density units (RDUs) of the white bands normalized to protein content (inset shows representative zymogram, with lane numbers corresponding to each RDU bar in the graph). MMP-2 and MMP-9 were identified according to their migration distance and apparent molecular weights. Unimplanted fresh carotid artery (fresh), alkali-purified elastin scaffolds (control) and 0.3% PGG-stabilized elastin scaffolds (PGG) were also analyzed in parallel with the explants. (**E**) Content of glycosaminoglycans (GAGs) in explants was measured and reported as ug/mg of extracted total protein. Unimplanted fresh carotid artery (fresh), alkali-purified elastin scaffolds (control), and 0.3% PGG-stabilized elastin scaffolds (PGG) were also analyzed in parallel with the explants. Color images available online at www.liebertonline.com/ten.

cellular components. Several approaches have been reported in the literature for decellularization, most of which use detergents and enzymes. We showed previously that detergent-decellularized arteries have a limited potential for repopulation with cells *in vitro*[46] and *in vivo*.[47] We hypothesized that the presence of the dense collagen–elastin network of fibers is responsible for the lack of experimental cell repopulation. To test that hypothesis, we treated decellularized arteries with collagenase and improved cell infiltration but also significantly changed mechanical properties of the

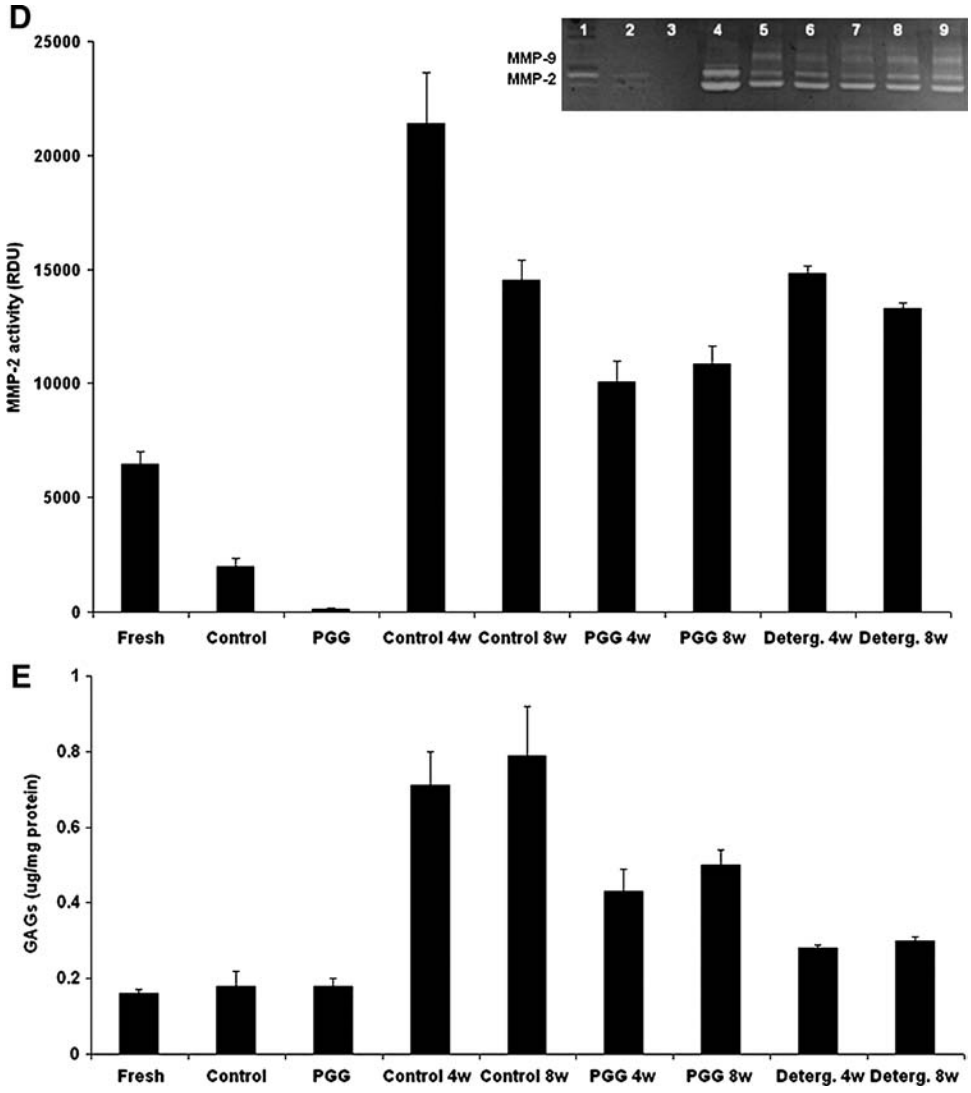

FIG. 6. (*Continued*).

scaffolds.[47] Because elastin regenerates slowly in tissue-engineered constructs, our goal was to obtain porous, cell- and collagen-free vascular elastin scaffolds from porcine carotid arteries and use them as building blocks for small-diameter vascular grafts. We screened several methods for elastin purification and eventually chose to use the NaOH extraction method, which was compared with a traditional detergent-based method.

Alkaline-extracted carotid arteries showed complete lack of cells according to histology and DNA analysis and almost complete collagen removal while maintaining elastin and proteoglycans intact. Most but not all intrinsic MMP activity was removed using decellularization. The tubular porous scaffolds maintained a cylindrical architecture, were capable of supporting their own weight, and were easy to handle and suture. The scaffolds were almost completely degraded by elastase *in vitro*, and their degradation products stimulated cell migration in a chemotaxis assay. Mechanical properties of the vascular elastin scaffolds, including tensile strength and distensibility, were similar to those of fresh arteries, but scaffolds exhibited lower burst pressure values and higher compliance, possibly because of loss of tissue collagen. Upon subdermal implantation, elastin scaffolds were readily infiltrated by activated fibroblasts and macrophages through the adventitia and intima layers but did not seem to have elicited significant immune reactions. Cell infiltration was continuous, and at 8 weeks, host cells infiltrating the scaffolds at high density populated almost 100% of scaffold thickness. Concomitant with cell infiltration, MMP levels rose, and there was gradual elastin degradation and deposition of collagen and proteoglycans.

Biological scaffolds, including those made of collagen and elastin, are prone to host enzymatic degradation. To gain control over *in vivo* degradation rates, we stabilized our elastin scaffolds with PGG, a polyphenol derived from plants. Our previous studies have demonstrated that polyphenols bind to elastin and in doing so renders it resistant to degradation.[42] By virtue of their elastin-binding properties, polyphenols also reduce calcification of glutaraldehyde-fixed bioprosthetic heart valves[38] and limit vascular degeneration associated with aneurysm formation and progression.[43] In our current studies, we hypothesized that, by delaying host tissue remodeling processes, we would help maintain vascular graft mechanical strength and patency for a longer period of time and allow for gradual remodeling to occur. PGG stabilized elastin scaffolds in a concentration-dependent manner, reduced distensibility,

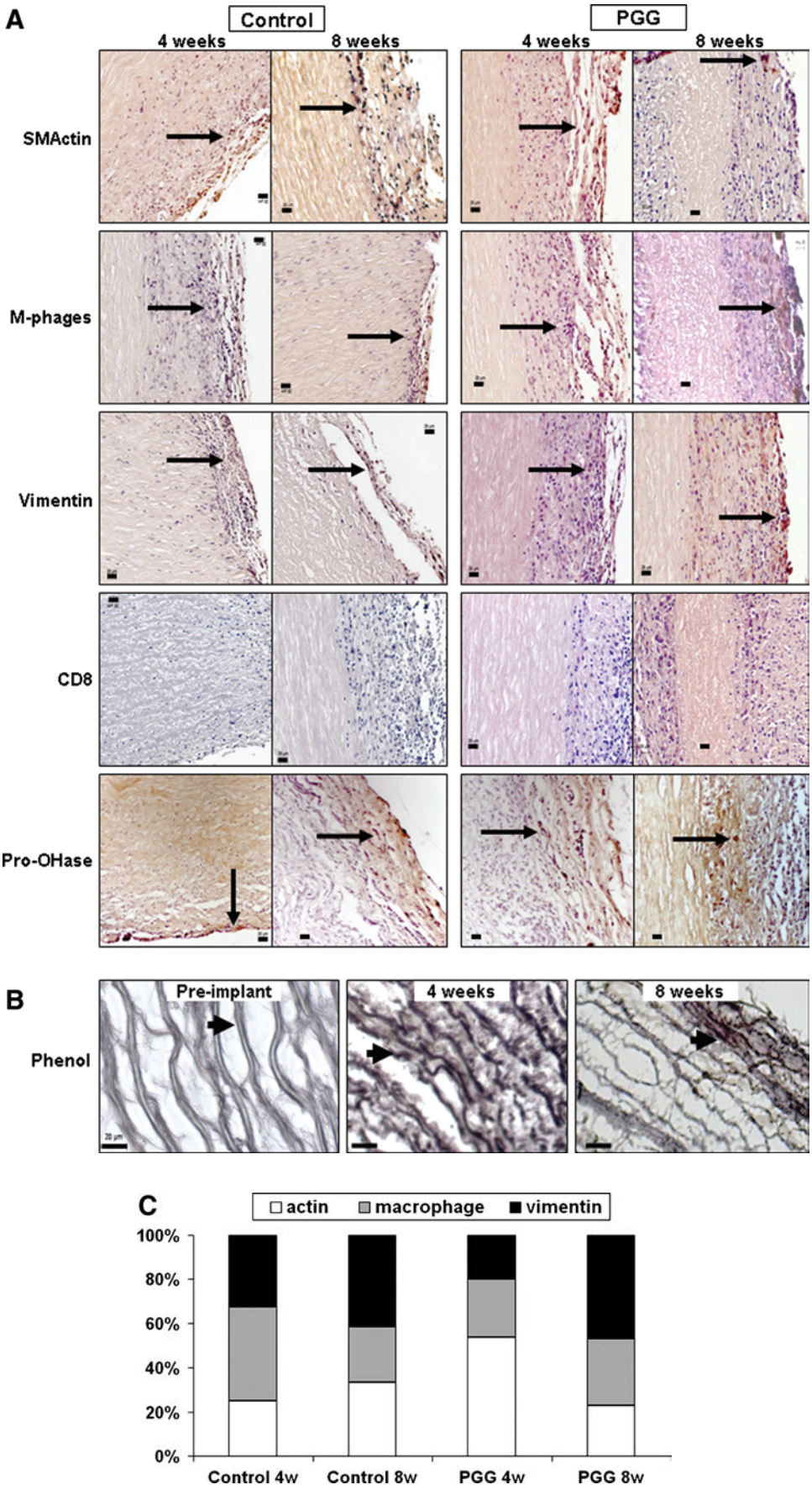

FIG. 7. (**A**) Immunohistochemical staining of cells infiltrating untreated elastin scaffolds (control) and 0.3% PGG stabilized elastin scaffolds (PGG) after 4 weeks and 8 weeks implantation. Sections were stained with antibodies to rat alpha-smooth muscle cell actin (SMActin), macrophages (M-phages), vimentin, cytotoxic lymphocytes (CD8), and prolyl-4-hydroxylase (Pro-OHase). Arrows point to one of many positive cells (dark brown). CD8 figure lacks arrows because no positive cells could be identified. Intima layer is toward the lower-right corner, and scale bars are 20 um in all sections. (**B**) Phenol staining showing elastin-bound PGG (dark brown) in PGG-fixed elastin scaffolds before implantation (left) and at 4 and 8 weeks after subdermal implantation. (**C**) Semi-quantitative analysis of cell type distribution within implants based on immunohistochemical staining of untreated elastin scaffolds (control) and 0.3% PGG-stabilized elastin scaffolds (PGG) after 4 weeks (4w) and 8 weeks (8w) of implantation. Numbers are expressed as percentage of total reactive cells. Color images available online at www.liebertonline.com/ten.

Table 1. Calcium Levels in Explanted Elastin Scaffolds

Sample	*Calcium content (μg/mg dry weight ± standard error of the mean)* 4 weeks	8 weeks
Control	103.27 ± 12.17^a	117.66 ± 12.01^b
Penta-galloyl glucose-treated	1.39 ± 0.22	4.47 ± 3.49
Detergent	0.59 ± 0.16^b	0.77 ± 0.05^b

[a]Statistical significance between time points within each fixation group ($p < 0.05$).
[b]Statistical significance between groups at each time point ($p < 0.05$).

and stiffened vascular elastin scaffolds but did not influence overall tensile strength or burst pressure and reduced compliance levels to physiologic levels, indicating that PGG-treated elastin scaffolds may have adequate properties to be used as vascular arterial grafts. Host cells infiltrated the PGG-treated elastin scaffolds at a much lower rate than untreated scaffolds, indicating that elastin stabilization possibly reduces cell infiltration. PGG-treated elastin fibers were found to degrade similarly to untreated fibers, albeit at a lower rate, and were replaced by new collagen fibers and higher levels of GAGs. Overall remodeling was correlated with MMP activities and presence of active prolyl-4-hydroxylase, enzymes involved in collagen degradation and synthesis, respectively.

Even after 8 weeks, the middle one-third of the PGG-treated implants still exhibited intact elastin fibers, whereas the outer two-thirds (corresponding to the intima and adventitia) were more collagenous in nature. This novel hybrid laminar structure may possess interesting mechanical properties that require further investigation. PGG-treated scaffolds did not appear to be cytotoxic *in vitro* and *in vivo*, because most host infiltrating cells interacted freely with PGG-treated elastin fibers. Apparently cell types did not differ between PGG-treated scaffolds and untreated scaffolds and were typically represented by activated fibroblasts and macrophages. PGG binding to elastin appeared to be stable over the 8-week study, as revealed by phenol stain, indicating that the bonds are stable under physiologic conditions, confirming some of our earlier *in vivo* observations.[43]

The third group of scaffolds investigated in this study were the detergent-decellularized arteries prepared using hypotonic shock, detergents, and nucleases that removed most cells but left vascular collagen and elastin fibers intact. These scaffolds showed similar susceptibility to elastase (when compared with the alkaline-extracted arteries), indicating that the decellularization procedure did not induce significant alterations in protein structure. Burst pressure of detergent-decellularized tissues was similar to those of fresh native arteries, suggesting that decellularization did not influence mechanical properties. Upon subdermal implantation, fibroblasts and macrophages infiltrated detergent-decellularized arteries, accounting for not more than 20% of total thickness (~10% from each side of the implant) at 4 weeks, without eliciting any detectable immune reactions. Cell infiltration did not progress with time of implantation, and cell numbers, density, and infiltration depths remained constant at 8 weeks, clearly showing that the density of the collagen–elastin network of fibers does not encourage cell infiltration and repopulation. Moreover, VVG and trichrome staining and GAG analysis did not reveal significant matrix remodeling in the implanted samples, which could be explained by the lower levels of cell infiltration in this model.

Limitations of this study include the need for more-detailed analysis of PGG–elastin interactions and their stability *in vivo*, the role of protease-inhibiting activities in tissue remodeling, and the role and source of host-infiltrating cells (derived from adjacent tissues or systemic sources) and long-term bioreactor studies and implantation of our scaffolds as vascular grafts. Subdermal implantation has been extensively used for testing cardiovascular biomaterials as it anticipates bioreactor and intra-vascular graft implantation experiments.[48–55] The subdermal milieu is adequate for evaluation of basic implant properties such as host cell infiltration, degeneration and remodeling, toxicity and biocompatibility, inflammation, and calcification.[52,53] Moreover, FDA and ISO standards clearly mandate subdermal implantation as a required test for cardiovascular devices, before implantation in large animals.[54,55] Ongoing studies in our group are testing the patency and usefulness of these tubular scaffolds as interposition vascular grafts in a circulatory model in large animals. These tubular scaffolds could be used in the future as by-pass shunts for myocardial and limb revascularization and as fistulae for dialysis access.

Conclusions

Alkali-purified, tubular elastin scaffolds exhibit many desirable biological and mechanical properties to be recommended for clinical applications as tissue-engineered vascular grafts. The scaffolds benefit from the natural architecture of the artery, are fully acellular nad very manageable, and exhibit high resistance to burst pressures and adequate compliance but also are readily degradable *in vivo*. Although elastin degradation products are chemotactic to vascular cells, hasty degradation of scaffolds may not be desired for vascular graft applications. Treatment with PGG reduces the rate of elastin biodegradation *in vitro* and thus may allow for control of *in vivo* biodegradation. Despite elastin stabilization, PGG-treated elastin encourages inward cell infiltration, elastin degradation, and matrix remodeling and inhibits calcification *in vivo*. These scaffolds are clearly superior to detergent-decellularized arteries in terms of cell infiltration and remodeling potential. Interactions between PGG and elastin are strong, and thus the beneficial effects of PGG could be maintained in the long term.

Acknowledgments

This work was funded in part by NIH Grants P20 RR-016461 and HL084194. C.S. was funded through NSF Grant EEC 0609035. The authors wish to thank Linda Jenkins for help with histology and the Godley-Snell Animal Research Center at Clemson University for animal studies.

References

1. Kasp-Grochowska, E., Kingston, D., and Glynn, L.E. Immunology of bovine heart valves. II. Reaction with connective tissue components. Ann Rheum Dis **31,** 290, 1972.
2. Berger, K., Sauvage, L.R., Rao, A.M., and Wood, S.J. Healing of arterial prostheses in man: its incompleteness. Ann Surg **175,** 118, 1972.

3. Debakey, M.E., Jordan, G.L., Jr., Abbott, J.P., Halpert, B., and O'Neal, R.M. The fate of Dacron vascular grafts. Arch Surg **89,** 757, 1964.
4. Szilagyi, D.E., Smith, R.F., Elliott, J.P., and Allen, H.M. Long-term behavior of a Dacron arterial substitute: clinical, roentgenologic and histologic correlations. Ann Surg **162,** 453, 1965.
5. Wesolowski, S.A., Fries, C.C., Hennigar, G., Fox, L.M., Sawyer, P.N., and Sauvage, L.R. Factors contributing to long-term failures in human vascular prosthetic grafts. J Cardiovasc Surg (Torino) **5,** 544, 1964.
6. Katsuyama, T., and Spicer, S.S. Histochemical differentiation of complex carbohydrates with variants of the concanavalin A-horseradish peroxidase method. J Histochem Cytochem **26,** 233, 1978.
7. Konner, K. Vascular access in the 21st century. J Nephrol **15 Suppl 6,** S28, 2002.
8. Weintraub, W.S., Jones, E.L., Craver, J.M., and Guyton, R.A. Frequency of repeat coronary bypass or coronary angioplasty after coronary artery bypass surgery using saphenous venous grafts. Am J Cardiol **73,** 103, 1994.
9. Williams, S.K., Rose, D.G., and Jarrell, B.E. Microvascular endothelial cell sodding of ePTFE vascular grafts: improved patency and stability of the cellular lining. J Biomed Mater Res **28,** 203, 1994.
10. Langer, R., and Vacanti, J.P. Tissue engineering. Science **260,** 920, 1993.
11. Nerem, R.M., and Seliktar, D. Vascular tissue engineering. Annu Rev Biomed Eng **3,** 225, 2001.
12. Shin'oka, T., Imai, Y., and Ikada, Y. Transplantation of a tissue-engineered pulmonary artery. N Engl J Med **344,** 532, 2001.
13. Shin'oka, T., Matsumura, G., Hibino, N., Naito, Y., Watanabe, M., Konuma, T., Sakamoto, T., Nagatsu, M., and Kurosawa, H. Midterm clinical result of tissue-engineered vascular autografts seeded with autologous bone marrow cells. J Thorac Cardiovasc Surg **129,** 1330, 2005.
14. Laflamme, K., Roberge, C.J., Pouliot, S., D'Orleans-Juste, P., Auger, F.A., and Germain, L. Tissue-engineered human vascular media produced *in vitro* by the self-assembly approach present functional properties similar to those of their native blood vessels. Tissue Eng **12,** 2275, 2006.
15. L'Heureux, N., Paquet, S., Labbe, R., Germain, L., and Auger, F.A. A completely biological tissue-engineered human blood vessel. Faseb J **12,** 47, 1998.
16. Cho, S.W., Lim, S.H., Kim, I.K., Hong, Y.S., Kim, S.S., Yoo, K.J., Park, H.Y., Jang, Y., Chang, B.C., Choi, C.Y., Hwang, K.C., and Kim, B.S. Small-diameter blood vessels engineered with bone marrow-derived cells. Ann Surg **241,** 506, 2005.
17. L'Heureux, N., Dusserre, N., Konig, G., Victor, B., Keire, P., Wight, T.N., Chronos, N.A., Kyles, A.E., Gregory, C.R., Hoyt, G., Robbins, R.C., and McAllister, T.N. Human tissue-engineered blood vessels for adult arterial revascularization. Nat Med **12,** 361, 2006.
18. Schaner, P.J., Martin, N.D., Tulenko, T.N., Shapiro, I.M., Tarola, N.A., Leichter, R.F., Carabasi, R.A., and Dimuzio, P.J. Decellularized vein as a potential scaffold for vascular tissue engineering. J Vasc Surg **40,** 146, 2004.
19. Niklason, L.E., Abbott, W., Gao, J., Klagges, B., Hirschi, K.K., Ulubayram, K., Conroy, N., Jones, R., Vasanawala, A., Sanzgiri, S., and Langer, R. Morphologic and mechanical characteristics of engineered bovine arteries. J Vasc Surg **33,** 628, 2001.
20. Guan, J., Sacks, M.S., Beckman, E.J., and Wagner, W.R. Synthesis, characterization, and cytocompatibility of elastomeric, biodegradable poly(ester-urethane)ureas based on poly(caprolactone) and putrescine. J Biomed Mater Res **61,** 493, 2002.
21. Nieponice, A., Soletti, L., Guan, J., Deasy, B.M., Huard, J., Wagner, W.R., and Vorp, D.A. Development of a tissue-engineered vascular graft combining a biodegradable scaffold, muscle-derived stem cells and a rotational vacuum seeding technique. Biomaterials **29,** 825, 2008.
22. Kuberka, M., Heschel, I., Glasmacher, B., and Rau, G. Preparation of collagen scaffolds and their applications in tissue engineering. Biomed Tech (Berl) **47 Suppl 1 Pt 1,** 485, 2002.
23. van Luyn, M.J., Plantinga, J.A., Brouwer, L.A., Khouw, I.M., de Leij, L.F., and van Wachem, P.B. Repetitive subcutaneous implantation of different types of (biodegradable) biomaterials alters the foreign body reaction. Biomaterials **22,** 1385, 2001.
24. Badylak, S.F. Xenogeneic extracellular matrix as a scaffold for tissue reconstruction. Transpl Immunol **12,** 367, 2004.
25. Liu, S.Q., Tieche, C., and Alkema, P.K. Neointima formation on vascular elastic laminae and collagen matrices scaffolds implanted in the rat aortae. Biomaterials **25,** 1869, 2004.
26. Feng, Z., Yamato, M., Akutsu, T., Nakamura, T., Okano, T., and Umezu, M. Investigation on the mechanical properties of contracted collagen gels as a scaffold for tissue engineering. Artif Organs **27,** 84, 2003.
27. Vorp, D.A., Maul, T., and Nieponice, A. Molecular aspects of vascular tissue engineering. Front Biosci **10,** 768, 2005.
28. Jaques, A., and Serafini-Fracassini, A. Morphogenesis of the elastic fiber: an immunoelectronmicroscopy investigation. J Ultrastruct Res **92,** 201, 1985.
29. Hafemann, B., Ensslen, S., Erdmann, C., Niedballa, R., Zuhlke, A., Ghofrani, K., and Kirkpatrick, C.J. Use of a collagen/elastin-membrane for the tissue engineering of dermis. Burns **25,** 373, 1999.
30. Kim, B.S., Baez, C.E., and Atala, A. Biomaterials for tissue engineering. World J Urol **18,** 2, 2000.
31. Itoh, H., Aso, Y., Furuse, M., Noishiki, Y., and Miyata, T. A honeycomb collagen carrier for cell culture as a tissue engineering scaffold. Artif Organs **25,** 213, 2001.
32. Park, S.N., Lee, H.J., Lee, K.H., and Suh, H. Biological characterization of EDC-crosslinked collagen-hyaluronic acid matrix in dermal tissue restoration. Biomaterials **24,** 1631, 2003.
33. Park, S.N., Park, J.C., Kim, H.O., Song, M.J., and Suh, H. Characterization of porous collagen/hyaluronic acid scaffold modified by 1-ethyl-3-(3-dimethylaminopropyl) carbodiimide cross-linking. Biomaterials **23,** 1205, 2002.
34. Pei, M., Seidel, J., Vunjak-Novakovic, G., and Freed, L.E. Growth factors for sequential cellular de- and re-differentiation in tissue engineering. Biochem Biophys Res Commun **294,** 149, 2002.
35. Goldstein, S., Clarke, D.R., Walsh, S.P., Black, K.S., and O'Brien, M.F. Transpecies heart valve transplant: advanced studies of a bioengineered xeno-autograft. Ann Thorac Surg **70,** 1962, 2000.
36. Kielty, C.M., Sherratt, M.J., and Shuttleworth, C.A. Elastic fibres. J Cell Sci **115,** 2817, 2002.
37. Fornieri, C., Quaglino, D., Jr., and Mori, G. Role of the extracellular matrix in age-related modifications of the rat aorta. Ultrastructural, morphometric, and enzymatic evaluations. Arterioscler Thromb **12,** 1008, 1992.
38. Isenburg, J.C., Simionescu, D.T., and Vyavahare, N.R. Tannic acid treatment enhances biostability and reduces

calcification of glutaraldehyde fixed aortic wall. Biomaterials **26,** 1237, 2005.
39. Charlton, A.J., Baxter, N.J., Lilley T.H., Haslam, E., McDonald, C.J., and Williamson, M.P. Tannin interactions with a full-length human salivary proline-rich protein display a stronger affinity than with single proline-rich repeats. FEBS Lett **382,** 289, 1996.
40. Luck, G., Liao, H., Murray, N.J., Grimmer, H.R., Warminski, E.E., Williamson, M.P., Lilley, T.H., and Haslam, E. Polyphenols, astringency and proline-rich proteins. Phytochemistry **37,** 357, 1994.
41. Haslam, E. Vegetable tannins—lessons of a phytochemical lifetime. Phytochemistry **68,** 2713, 2007.
42. Isenburg, J.C., Simionescu, D.T., and Vyavahare, N.R. Elastin stabilization in cardiovascular implants: improved resistance to enzymatic degradation by treatment with tannic acid. Biomaterials **25,** 3293, 2004.
43. Isenburg, J.C., Simionescu, D.T., Starcher, B.C., and Vyavahare, N.R. Elastin stabilization for treatment of abdominal aortic aneurysms. Circulation **115,** 1729, 2007.
44. Isenburg, J.C., Karamchandani, N.V., Simionescu, D.T., and Vyavahare, N.R. Structural requirements for stabilization of vascular elastin by polyphenolic tannins. Biomaterials **27,** 3645, 2006.
45. Bailey, M.T., Pillarisetti, S., Xiao, H., and Vyavahare, N.R. Role of elastin in pathologic calcification of xenograft heart valves. J Biomed Mater Res A **66,** 93, 2003.
46. Lu, Q., Ganesan, K., Simionescu, D.T., and Vyavahare, N.R. Novel porous aortic elastin and collagen scaffolds for tissue engineering. Biomaterials **25,** 5227, 2004.
47. Simionescu, D.T., Lu, Q., Song, Y., Lee, J.S., Rosenbalm, T.N., Kelley, C., and Vyavahare, N.R. Biocompatibility and remodeling potential of pure arterial elastin and collagen scaffolds. Biomaterials **27,** 702, 2006.
48. Connolly, J.M., Alferiev, I., Clark-Gruel, J.N., Eidelman, N., Sacks, M., Palmatory, E., Kronsteiner, A., Defelice, S., Xu, J., Ohri, R., Narula, N., Vyavahare, N., and Levy, R.J. Triglycidylamine crosslinking of porcine aortic valve cusps or bovine pericardium results in improved biocompatibility, biomechanics, and calcification resistance: chemical and biological mechanisms. Am J Pathol **166,** 1, 2005.
49. Fischlein, T., and Fasol, R. *In vitro* endothelialization of bioprosthetic heart valves. J Heart Valve Dis **5,** 58, 1996.
50. Ganta, S.R., Piesco, N.P., Long, P., Gassner, R., Motta, L.F., Papworth, G.D., Stolz, D.B., Watkins, S.C., and Agarwal, S. Vascularization and tissue infiltration of a biodegradable polyurethane matrix. J Biomed Mater Res A **64,** 242, 2003.
51. Golomb, G., and Ezra, V. Prevention of bioprosthetic heart valve tissue calcification by charge modification: effects of protamine binding by formaldehyde. J Biomed Mater Res **25,** 85, 1991.
52. Hinds, M.T., Courtman, D.W., Goodell, T., Kwong, M., Brant-Zawadzki, H., Burke, A., Fox, B.A., and Gregory, K.W. Biocompatibility of a xenogenic elastin-based biomaterial in a murine implantation model: the role of aluminum chloride pretreatment. J Biomed Mater Res A **69,** 55, 2004.
53. Liu, G.F., He, Z.J., Yang, D.P., Han, X.F., Guo, T.F., Hao, C.G., Ma, H., and Nie, C.L. Decellularized aorta of fetal pigs as a potential scaffold for small diameter tissue engineered vascular graft. Chin Med J (Engl) **121,** 1398, 2008.
54. Maluf-Meiken, L.C., Silva, D.R., Duek, E.A., and Alberto-Rincon, M.C. Morphometrical analysis of multinucleated giant cells in subdermal implants of poly-lactic acid in rats. J Mater Sci Mater Med **17,** 481, 2006.
55. Sacks, M.S., Hamamoto, H., Connolly, J.M., Gorman, R.C., Gorman, J.H., 3rd, and Levy, R.J. *In vivo* biomechanical assessment of triglycidylamine crosslinked pericardium. Biomaterials **28,** 5390, 2007.

Address correspondence to:
Dan T. Simionescu, Ph.D.
Biocompatibility and Tissue Regeneration Laboratory
Department of Bioengineering
Clemson University
501 Rhodes Engineering Research Center
Clemson, SC 29634

E-mail: dsimion@clemson.edu

Received: July 13, 2008
Accepted: February 27, 2009
Online Publication Date: April 9, 2009